Acta Biomaterialia 143 (2022) 253–265

Contents lists available at ScienceDirect

Acta Biomaterialia

journal homepage: www.elsevier.com/locate/actbio

Full length article

Pre-culture of human mesenchymal stromal cells in spheroids facilitates chondrogenesis at a low total cell count upon embedding in biomaterials to generate cartilage microtissues

Flurina Staubli[a,b,c], Martin J. Stoddart[a], Matteo D'Este[a,*], Andrea Schwab[a,d,e]

[a] AO Research Institute Davos, Clavadelerstrasse 8, Davos 7270, Switzerland
[b] Department of Oral Maxillofacial Surgery and Special Dental Care, University Medical Center Utrecht, Utrecht University, Utrecht, the Netherlands
[c] Regenerative Medicine Center Utrecht, Utrecht, the Netherlands
[d] Department of Oral and Maxillofacial Surgery, Erasmus MC, University Medical Center Rotterdam, the Netherlands
[e] Department of Orthopaedics and Sports Medicine, Erasmus MC, University Medical Center Rotterdam, the Netherlands

ARTICLE INFO

Article history:
Received 8 October 2021
Revised 21 February 2022
Accepted 24 February 2022
Available online 1 March 2022

Keywords:
Mesenchymal stromal cells
Spheroid
Chondrogenic differentiation
Collagen
Hyaluronan
Biomaterials

ABSTRACT

Material-assisted cartilage tissue engineering has limited application in cartilage treatment due to hypertrophic tissue formation and high cell counts required. This study aimed at investigating the potential of human mesenchymal stromal cell (hMSC) spheroids embedded in biomaterials to study the effect of biomaterial composition on cell differentiation. Pre-cultured (3 days, chondrogenic differentiation media) spheroids (250 cells/spheroid) were embedded in tyramine-modified hyaluronic acid (THA) and collagen type I (Col) composite hydrogels (four combinations of THA (12.5 vs 16.7 mg/ml) and Col (2.5 vs 1.7 mg/ml) content) at a cell density of 5×10^6 cells/ml (2×10^4 spheroids/ml). Macropellets derived from single hMSCs (2.5×10^5 cells, ScMP) or hMSC spheroids (2.5×10^5 cells, 10^3 spheroids, SpMP) served as control. hMSC differentiation was analyzed using glycosaminoglycan (GAG) quantification, gene expression analysis and (immuno-)histology. Embedding of hMSC spheroids in THA-Col induced chondrogenic differentiation marked by upregulation of aggrecan (ACAN) and COL2A1, and the production of GAGs . Lower THA led to more pronounced chondrogenic phenotype compared to higher THA content. Col content had no significant influence on hMSC chondrogenesis. Pellet cultures showed an upregulation in chondrogenic-associated genes and production of GAGs with less upregulation of hypertrophic-associated genes in SpMP culture compared to ScMP group. This study presents hMSC pre-culture in spheroids as promising approach to study chondrogenic differentiation after biomaterial encapsulation at low total cell count (5×10^6/ml) without compromising chondrogenic matrix production. This approach can be applied to assemble microtissues in biomaterials to generate large cartilage construct.

Statement of significance

In vitro studies investigating the chondrogenic potential of biomaterials are limited due to the low cell-cell contact of encapsulated single cells. Here, we introduce the use of pre-cultured hMSC spheroids to study chondrogenesis upon encapsulation in a biomaterial. The use of spheroids takes advantage of the high cell-cell contact within each spheroid being critical in the early chondrogenesis of hMSCs. At a low seeding density of $5{\cdot}10^6$ cells/ml (2×10^4 spheroids/ml) we demonstrated hMSC chondrogenesis and cartilaginous matrix deposition. Our results indicate that the pre-culture might have a beneficial effect on hypertrophic gene expression without compromising chondrogenic differentiation. This approach has shown potential to assemble microtissues (here spheroids) in biomaterials to generate large cartilage constructs and to study the effect of biomaterial composition on cell alignment and migration.

* Corresponding author.
E-mail address: matteo.deste@aofoundation.org (M. D'Este).

https://doi.org/10.1016/j.actbio.2022.02.038

1. Introduction

Articular cartilage is damaged as a consequence of trauma, ageing or degenerative joint disease [1]. Due to its poor cellularization accounting for only 2% of the cartilage volume [2] and the absence of vascularization, cartilage has little capacity for spontaneous repair [3]. This poor intrinsic healing potential can lead to the formation of fibrocartilaginous tissue, which fails over time and leads to impaired joint function and disability [4]. Currently used clinical treatment procedures like mosaicplasty, microfracture or autologous chondrocyte implantation (ACI) fail to restore the native structure and function of damaged articular cartilage and can also lead to donor site morbidity [5,6]. The latest generation of (matrix associated) ACI using chondrocyte pellets (chondrosphere/Spherox, CO.DON AG) has shown promising outcomes in the treatment of large chondral defects in the knee [7–9]. This indicates that high cell density and cell-cell contacts encountered by cells inside pellets is sufficient to maintain chondrocyte phenotype even at low total cell count, as found in previous studies [10,11]. Another approach to treat cartilage defects is based on tissue engineering cartilage constructs from stem cells *in vitro* before implantation into a cartilage defect. Macropellet cultures are the current gold standard to differentiate hMSCs towards chondrogenic lineage *in vitro* [12]. However, the macropellet culture presents several drawbacks mostly related to the construct up-scaling and hypertrophic differentiation of hMSCs followed by pre-mineralization of the generated cartilage tissue [13]. This is marked by an upregulation of, among others, collagen type X (COL10A1) and deposition of mineralized tissue. Optimal conditions for pellet cultures, for example cell number, cell density and oxygen concentration, have been discussed in literature. Recent studies found that the reduction of pellet size can improve chondrogenesis [14,15]. In a previous study, micropellets (170 cells/pellet) cultured under low oxygen environment resulted in higher chondrogenesis, accompanied by an increase in Col10A1 deposition, compared to bigger pellets (2×10^5 cells/pellet) [15].

Biomaterial based approaches have the advantage to provide a 3D environment and filling of larger defect volumes. Biomaterials have been shown to influence the phenotype, adhesion, migration, proliferation, and differentiation of cells, and might present a better culture environment in terms of chondrogenesis and/or hypertrophic differentiation of hMSCs compared to standard macropellet culture [16]. Hydrogels are an attractive class of biomaterials due to their similarities to the native extracellular matrix (ECM), namely the high water content, biodegradability, porosity, and biocompatibility [17,18]. Hyaluronan (HA) and Collagen type I (Col) are both major components of the native connective tissue ECM. Col can form fibrillar hydrogels upon neutralization and possesses cell adhesion sequences, both promoting cell attachment and infiltration. However, Col based hydrogels typically display poor mechanical properties, as well as rapid shrinking and degradation [19–21]. HA in turn can form a matrix with viscoelastic properties like the native ECM, e.g., after functionalization with tyramine (THA). THA can be enzymatically cross-linked by horseradish peroxidase (HRP) and hydrogen peroxide (H_2O_2) under mild conditions, allowing for good cell viability as opposed to most physical cross-linking methods [22–24]. Functionalization of biopolymers with tyrosine increased bond strength to native cartilage tissue thus indicating an enhanced biomaterial-tissue integration [25]. It was shown in a previous study, that THA-Col composite biomaterials can achieve homogeneous biomaterial distribution, retain mechanical properties of THA without inhibiting Col fibrillogenesis and allow for cell encapsulation with good viability [22–24]. After cell encapsulation in biomaterials, cells often show a low chondrogenic differentiation potential, possibly accompanied by local matrix deposition around the cells rather than homogenously distributed throughout the scaffold [26,27]. Cell embedding in biomaterials requires high cell numbers of more than 10^7 cells per ml of scaffold volume [28], some studies even showing that up to 10^8 cells per ml of scaffold volume leads to the best chondrogenic outcome [29]. This cell number is dependent on the biomaterial and should be optimized to aim for optimal conditions. While a biomaterial provides a 3D environment which is beneficial to fill a large cartilage defect volume, the high cell number required for seeding the defect volume and insufficient cartilaginous matrix production remains a major drawback in biomaterial-based approaches. Given the fact that the high cell density and cell-cell interactions are critical factors in early *in vitro* hMSC chondrogenesis [30], the embedding of pre-cultured hMSC spheroids represents a promising approach to overcome inhomogeneous matrix deposition in scaffolds and high cell numbers required to upscale biomaterial-based cartilage constructs.

The aim of this study was to characterize the effect of hMSC pre-culture in spheroids (250 cells/spheroid) in chondrogenic differentiation media containing transforming growth factor beta (TGF-β1) before embedding in THA-Col hydrogels at four compositions. We hypothesized that the initial high cell-cell contact of hMSCs inside the spheroids together with 3 days of priming with TGF-β1 stimulates the chondrogenic differentiation potential of the hMSCs even when seeded at a low total cell count of 5×10^6 cells per ml of hydrogel. In a second study, spheroids were assembled into macropellets (SpMP: 2.5×10^5 cells/SpMP; 10^3 spheroids/SpMP) and compared to the gold standard, the standard macropellet generated from single cells (ScMP: 2.5×10^5 cells/ ScMP). This set up aimed to investigate whether the short-term priming (3 days) of hMSC spheroids influenced chondrogenic differentiation of hMSCs in pellet culture (Fig. 1).

Chondrogenic differentiation was analyzed using quantitative reverse transcription polymer chain reaction (RT-qPCR), (immuno-) histological stainings and quantification of deposited glycosaminoglycans (GAGs).

2. Materials and methods

2.1. Biomaterial preparation and characterization

2.1.1. THA synthesis

HA was conjugated with tyramine as described by Loebel et al [31]. HA (280–290 kDa, 5 mM carboxylic groups; Contipro Biotech S.R.O) was functionalized through addition of 4-(4,6-dimethoxy-1,3,55-triazin-2-yl)-4-mehtyl-morpholinium chloride and tyramine at a stoichiometric ratio of 1:1:1 and subsequent mixing for 24 h at 37°C. THA was precipitated by dropwise addition of ethanol (96% v/v) and subsequent drying. The degree of substitution of the THA (Batch number 797-46) was 5.26% as determined by reading the absorbance at 275 nm (MultiskanGo™, Thermo Fisher Scientific).

2.1.2. THA-Col hydrogel preparation

THA was exposed to UV light (30 min) and reconstituted at a final concentration of 25 mg/ml (overnight at 4°C under agitation) in phosphate buffered saline (PBS, Sigma-Aldrich) for rheological characterization or in high glucose Dulbecco's modified eagle media (DMEM HG, Gibco) for cell culture experiments containing 0.3 or 0.5 U/ml horseradish peroxidase (HRP, Sigma-Aldrich). Enzymatic cross-linking was initiated by hydrogen peroxide (H_2O_2, Roth) at final concentrations ranging from 2 - 24 ppm and incubated for 30 min at 37°C to initiate the enzymatic gelation. For additional light cross-linking, eosin Y (2 mg/ml eosin Y in dimethyl sulfoxide, Sigma-Aldrich) was added at final concentrations of 0.02 mg/ml before enzymatic cross-linking. THA-Col composites were prepared by mixing reconstituted THA and Col (initial concentration: 5 mg/ml, rat tail collagen I in 0.2% v/v acetic acid, Corning) at

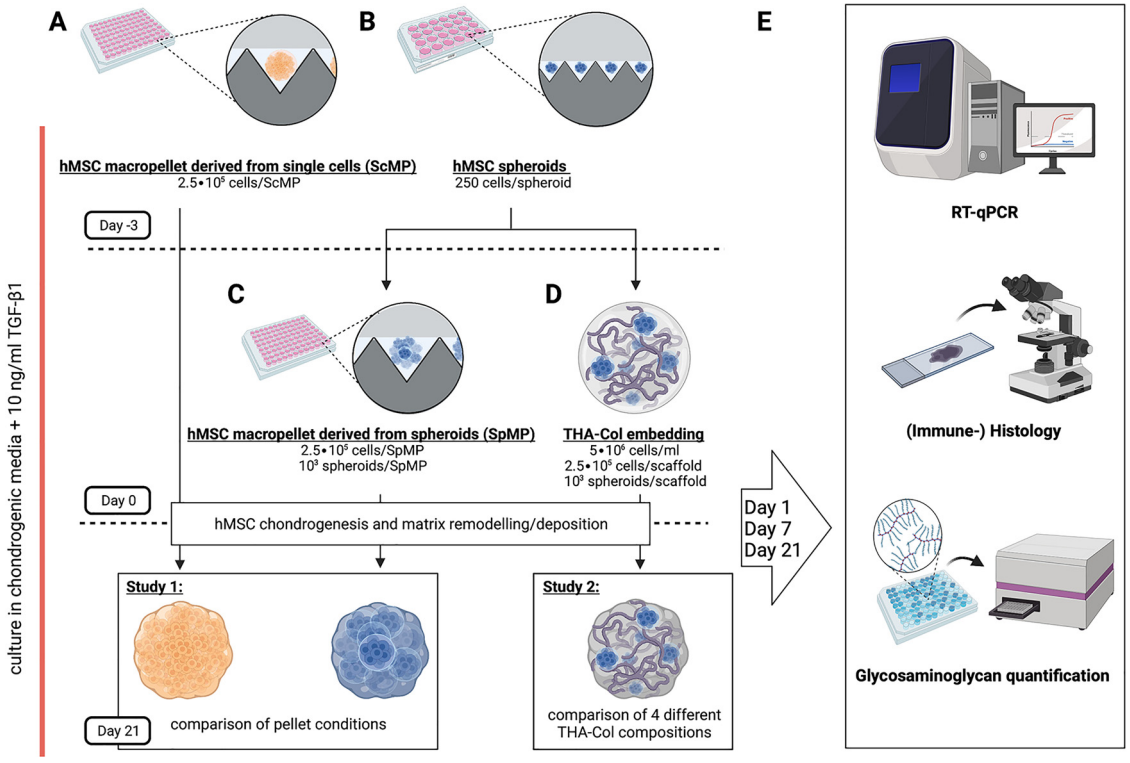

Fig. 1. Experimental overview of hMSC chondrogenesis in standard single cell derived macropellets (ScMP), spheroid derived macropellets (SpMP) and spheroids embedded in THA-Col hydrogels. (A) 2.5 × 10^5 hMSCs were cultured as ScMP (in chondrogenic media + TGF-β1) for a total of 24 days. (B) 250 hMSCs were pre-cultured as spheroids (in chondrogenic media + TGF-β1) for 3 days. (C) Pre-cultured spheroids were assembled into SpMPs (2.5 × 10^5 cells) and cultured in chondrogenic media + TGF-β1 for further 21 days. (D) Pre-cultured spheroids were embedded in THA-Col hydrogels (5 × 10^6 cells/ml) and cultured in chondrogenic media + TGF-β1 for further 21 days. (E) Chondrogenesis of hMSCs under different culture conditions was evaluated on day 1, 7 and 21 by gene expression analysis (RT-qPCR), (immuno-) histological stainings and glycosaminoglycan (GAG) quantification.

Table 1
Overview of the THA-Col compositions. The polymer concentrations refer to the final concentration in the THA-Col composite. T, THA: Tyramine modified hyaluronic acid. C, Col: collagen I.

Material		THA [mg/ml]	Col [mg/ml]
T12.5-C2.5	THA low	12.5	2.5
T12.5-C1.7		12.5	1.7
T16.7-C2.5	THA high	16.7	2.5
T16.7-C1.7		16.7	1.7

different polymer compositions as summarized in Table 1. To induce Col gelation parallel to enzymatic gelation of THA, the hydrogel precursor was neutralized to pH 7. Concentrations of H_2O_2 and HRP (indicated in respective sections in brackets) are always given relative to the THA volume within the composite. To further increase shape fidelity of the samples enzymatically crosslinked hydrogels were exposed to green light at the 3D Discovery workstation interface (light curing Kit 505 nm, 200 mW/cm^2, RegenHu).

2.1.3. Rheological characterization of biomaterials

Visco-elastic properties of the biomaterials were analyzed using the Anton-Paar MCR-302 rheometer with a 25-1 cone-plate geometry and a gap distance of 0.049 mm at 20°C. Silicone oil (Sigma-Aldrich) was applied to prevent the samples (enzymatically cross-linked (E CL) and additionally light cross-linked (E + L CL)) from drying out during the measurements. Amplitude sweeps (frequency = 1 Hz, amplitude = 0.01 – 100% strain) were performed to characterize the shear moduli and the visco-elastic behavior of the hydrogels. All measurements were performed in triplicates.

2.2. Cell culture

2.2.1. hMSC isolation and expansion

hMSCs of 3 donors between the age of 48 and 62 years were isolated from bone marrow aspirates as described before [32] with full ethical approval (Inselspital Bern - Bern Req-2016-00141, University hospital Freiburg - EKFreiburg: 135/14). hMSCs were subcultured (3 × 10^5 cells/cm^2) in growth media composed of Minimal Essential Media (aMEM, Gibco), 10% v/v fetal bovine serum (FBS, Corning), 1% v/v Pen-Strep (100 U/ml of penicillin, 100 µg/ml of streptomycin, Gibco) and 5 ng/ml basic fibroblast growth factor (bFGF, Fitzgerald Industries International) at 37°C and 5% CO_2. The media was changed twice a week and the cells were sub-cultured at 80% confluency. Cells in passage 3 were used for chondrogenic differentiation (Fig. 1).

2.2.2. hMSC spheroid culture

To generate the spheroids, hMSCs (passage 3) were seeded in a 6-well microwell plate (Aggrewell 400, Stemcell Technology) according to the manufacturer's protocol using chondrogenic media (DMEM HG, 50 µg/ml ascorbic acid 2-phosphate (Sigma-Aldrich), 100 nM dexamethasone (Sigma-Aldrich), 1% v/v ITS+ premix (Corning), 1% v/v non-essential amino acids (MEM NEAA, Gibco), 10 ng/ml transforming growth factor beta (TGF-β1, Fitzgerald), 1% v/v Pen-Strep) and cultured for 3 days. Each spheroid contained approximately 250 hMSCs (Fig. 1).

2.2.3. MSC spheroid embedding in THA-Col biomaterials

After 3 days of pre-culture, hMSC spheroids were resuspended in chondrogenic media, mixed with the hydrogel precursors (Table 1) at a final concentration of 5 × 10^6 cells/ml

(2×10^4 spheroids/ml) containing TGF-β1. The hydrogels were enzymatically crosslinked (0.5 U/ml HRP, 24 ppm H_2O_2) in custom made silicone molds (diameter: 6 mm; height: 2 mm; volume: 50 µl) for 30 min at 37°C with subsequent light cross-linking (Light curing Kit 505 nm, RegenHu, 7 sec/sample). Samples were transferred into 24-well plates and cultured with chondrogenic media at 37°C and 5% CO_2 for 21 days. Media was changed three times a week.

2.2.4. Spheroid derived macropellets (SpMP)

Spheroids were harvested after 3 days of pre-culture and resuspended in chondrogenic media at 4000 spheroids/ml (10^6 cells/ml). 250 µl of the cell suspension (2.5×10^5 cells; 10^3 spheroids) were transferred into each well of a 96-well V-bottom non-tissue culture treated plate (Thermo Scientific). The plate was centrifuged (400 G, 5 min) and cultured in 250 µl chondrogenic media at 37°C and 5% CO_2 for 21 days (total culture time including pre-culture: 24 days). Media was changed three times a week.

2.2.5. Single cell derived macropellets (ScMP, gold standard)

To generate ScMPs, hMSCs (passage 3) were trypsinized and resuspended in chondrogenic media at 10^6 cells/ml. ScMPs cultured in chondro-permissive media (chondrogenic media without TGF-β1) were used as negative control. 2.5×10^5 cells were transferred in each well of a 96-well V-bottom non-tissue culture treated plate (Thermo Scientific) according to the protocol described before and cultured in 250 µl media at 37°C and 5% CO_2 for a total of 24 days. Media was changed three times a week.

2.3. Histological processing and staining

2.3.1. Cryo embedding of cell pellets and THA-Col samples

For histological stainings, hydrogel samples (day 1 and 21) and pellets (day 21) were harvested, washed with PBS and fixed with 4% neutral buffered formalin (24h, room temperature, Formafix AG). After washing with PBS (>24 h), the samples were processed with 15% sucrose (24 h), 30% sucrose (72 h), 30% sucrose mixed with tissue freezing media (Leica) in a 1:1 ratio (24 h) at 4°C and subsequently snap frozen in tissue freezing media in liquid nitrogen. Samples were cut to 8 µm slices using a cryostat microtome (HM 500 OM; Zeiss) and kept at -20°C until they were used for staining.

2.3.2. Safranin O-fast green staining

To visualize proteoglycans secreted by the hMSCs during chondrogenic differentiation in the hydrogel samples and pellet cultures (SpMP, ScMP), a safranin O staining was performed on methanol (100% v/v, 15 min at room temperature) fixed slides. The slides were washed with deionized water, stained with Weigert's hematoxylin (10 min; Sigma-Aldrich), blued with tap water (10 min), rinsed with deionized water, and stained with fast green (0.02% w/v; Sigma-Aldrich) for 6 min to visualize collagenous matrix (green). After washing with acetic acid (1% v/v; Fluka), the samples were incubated with safranin O (0.1% w/v, 15 min; Sigma-Aldrich) to stain proteoglycans (red). The staining was differentiated with ethanol (70%, 25 sec; Alcosuisse), subsequently dehydrated with a series of alcohols (96% ethanol , ethanol absolute (2x), xylene (2; Brenntag item)) and mounted with a coverslip (Eukitt, Sigma-Aldrich). Microscopic evaluation was performed using a bright-field microscope (Olympus BX63, Olympus).

2.3.3. Immuno-histochemistry

To visualize aggrecan and collagen II produced by hMSCs during chondrogenic differentiation, immuno-histochemical stainings were performed on methanol fixed samples. The slides were washed with deionized water and endogenous peroxidase activity was blocked with hydrogen peroxide (H_2O_2) in methanol (aggrecan: 0.3% v/v for 30 min, collagen II: 3% v/v for 20 min, followed by 100% methanol for 1 min). After washing with PBS-Tween (0.1%, Sigma-Aldrich), enzymatic demasking was performed using 25 mg/ml Hyaluronidase (Sigma-Aldrich) and 0.25 U/ml Chondroitinase ABC (Sigma-Aldrich) in PBS-Tween for 30 min at 37°C . For the aggrecan staining, slides were additionally incubated in reduction buffer (50 mM Trisma base, Sigma-Aldrich and 200 mM Sodium-chloride at pH 7.35, Sigma-Aldrich) containing 10 mM DTT (Sigma-Aldrich) for 2 h followed by an alkylation step (40 mM iodoacetamide (Sigma-Aldrich) in PBS) for 1 h. After washing, the slides were blocked with serum (horse serum for the aggrecan staining, goat serum for collagen II staining, both 1:20 diluted in PBS-Tween, Vector Laboratories) for 1 h at room temperature, then incubated with the primary antibody (aggrecan: 4 µg/ml, 12/21/1-C-6, Development Studies Hybridoma Bank (DSHB), collagen II: 2 µg/ml, CIICI, DSHB) diluted in PBS-Tween containing respective serum (1:200) overnight at 4°C. After washing with PBS-Tween, the slides were incubated with the secondary antibody (aggrecan: biotinylated Anti-Mouse IgG (H+L) 1:200 in PBS-Tween, Vector laboratories; collagen II: biotinylated Anti-rabbit IgG (H+L) 1:200 in PBS-Tween, Vector laboratories) for 30 min, followed by the ABC-complex (Vectastain Elite ABC kit, Vector laboratories) for 30 min at room temperature. ImmPACT DAB (LSBio) was applied to develop the brown color of the staining, followed by rinsing with deionized water (5 min), counterstaining with Mayer's hematoxylin (30 s) and blueing in tap water (5 min). Slides were dehydrated with a series of alcohols (50% ethanol, 70% ethanol, 96% ethanol, ethanol absolute, xylene (2x ;)) and sealed using a coverslip . Microscopic evaluation was performed using a bright-field microscope (Olympus BX63, Olympus).

2.4. Gene expression analysis: Real-Time Quantitative Polymerase Chain Reaction (RT-qPCR)

Total RNA was isolated from hydrogel samples and pellets (day 1, 7 and 21) using TriReagent® (Molecular Research Center Inc.) according to the manufacturer's protocol, including a high salt precipitation (Molecular Research Center Inc.) step. The RNA quantity was measured using the NanoDrop 1000 spectrophotometer (Thermo Fischer). cDNA synthesis of 1 µg RNA was performed using Vilo Superscript (Invitrogen) according to the manufacturer's instructions using a Thermocycler (Mastercycler gradient, Eppendorf). For RT-qPCR, 10 µl of reaction mixture containing 5 µl TaqMan Universal Master Mix (Thermo Fischer), primer and probes (forward and reverse primer: 900 nM each; TaqMan probe: 250 nM), diethylpyrocarbonate (DEPC) water, and cDNA (10 ng) was loaded on each well of a 384 well plates. A standard PCR program was run (2 min of initial heating to 50°C, 10 min at 95°C for polymerase activation and 40 cycles of alternating 95°C for 15 sec and 60°C for 1 min for denaturation and annealing). The relative gene expression of different genes was calculated in duplicates of each donor using the $2^{-\Delta\Delta Cq}$ method relative to the housekeeping gene ubiquitin C (UBC) and normalization to day 1 samples of the same condition and donor. The genes evaluated were the chondrogenic-associated genes aggrecan (ACAN), collagen type II (COL2A1) and SOX9, the fibrous- and hypertrophy-associated genes collagen type I (COL1A1) and collagen type X (COL10A1) and the osteoblast transcription factor RUNX2. Assay IDs of the assay on demand (ThermoFisher) and sequences of primer and probe genes are listed in Table 2.

2.5. Quantification of Glycosaminoglycans (GAG) and DNA

To quantify GAGs and DNA within pellets and hydrogels (day 1 and 21), the samples were lyophilized followed by proteinase K

Table 2
List of primer and probe sequences (forward, reverse and probe) and assay IDs (assays on demand) used for RT-qPCR.

Gene	Forward Primer	Reverse Primer	Probe
COL1A1	5'-CCC TGG AAA GAA TGG AGA TGA T-3'	5'-ACT GAA ACC TCT GTG TCC CTT CA-3'	5'-CGG GCA ATC CTC GAG CAC CCT -3'
COL2A1	5'-GGC AAT AGC AGG TTC ACG TAC A-3'	5'-GAT AAC AGT CTT GCC CCA CTT ACC-3'	5'-CCT GAA GGA TGG CTG CAC GAA ACA TAC-3'
COL10A1	5'-ACG CTG AAC GAT ACC AAA TG-3'	5'-TGC TAT ACC TTT ACT CTT TAT GGT GTA-3'	5'-ACT ACC CAA CAC CAA GAC ACA GTT CTT CAT TCC-3'
ACAN	5'-AGT CCT CAA GCC TCC TGT ACT CA-3'	5'-CGG GAA GTG GCG GTA ACA-3'	5'-CCG GAA TGG AAA CGT GAA TCA GAA TCA ACT-3'
RUNX2	5'-AGC AAG GTT CAA CGA TCT GAG AT-3'	5'-TTT GTG AAG ACG GTT ATG GTC AA-3'	5'-TGA AAC TCT TGC CTC GTC CAC TCC G-3'
UBC	Assay ID: Hs00824723_m1		
SOX9	Assay ID: Hs00165814_m1		

(0.5 mg/ml, Roche) digestion at 56°C. DNA content was measured using the Quant-iT^{TM} PicoGreen (ThermoFisher) assay according to the manufacturer's instructions. The fluorescence was measured (485 nm excitation, 535 nm emission wavelength, Tecan infinite 200 PRO, Tecan). A DNA standard curve was used to quantify the DNA content in the samples.

GAG content retained in the samples was determined using the dimethyl methylene blue (DMMB, pH 1.5, ThermoFisher) dye method. Absorbance measurement was read at 535 nm using a plate reader (Tecan infinite 200 PRO; Tecan). A chondroitin 4-sulfate sodium salt (Sigma-Aldrich) standard curve was generated to quantify the GAG content in the samples.

2.6. Statistical analysis

All cell culture experiments were performed with n=3 biological (3 Donors) and n=2 replicates (2 samples per group and time point) each. Material characterization was performed in triplicates. Results are displayed as single points/repeats including mean and standard deviation, or as bar plot showing mean and standard deviation. Fold-changes of PCR results are displayed as geometrical mean including geometrical standard deviation. Statistical analysis was performed using GraphPad Prism (Prism 8, USA). Two-way Analysis of Variance (ANOVA) including Tukey's multiple comparison test was applied. Statistical significance was assumed for p-values < 0.05.

3. Results

3.1. THA-Col biomaterial characterization

The biomaterial characterization of the cell-free and cell-laden THA-Col biomaterials is summarized in Fig. 2. Storage shear moduli of the four biomaterial formulations (Table 1) were measured at 1% strain of the amplitude sweep (cell-free). The enzymatically cross-linked (E CL) hydrogels showed a similar profile for the different THA-Col compositions. Increase in THA content led to a more pronounced increase in storage modulus than an increase in the Col content. After additional light cross-linking (E+L CL) of the hydrogels, the storage moduli (G') at 1% strain were in the same order of magnitude for all materials, ranging from 360 – 910 Pa, (Fig. 2A). Enzymatically and light cross-linked THA-Col (cell-free) showed swelling after 1 day in chondrogenic media. From day 1 on, the diameter of the samples stayed constant up to day 7 of incubation in media (Fig. 2B). A higher content of THA (16.7 mg/ml) in the composite led to more swelling, whereas the Col content showed only a minor effect on swelling behavior.

Brightfield images of spheroids embedded in THA-Col biomaterials (Fig. 2C) showed a faster cell migration out of the spheroids in the low THA group (12.5 mg/ml) compared to the high THA (16.6 mg/ml) content hydrogels on day 1. On day 7, more cell migration and interaction with the material was present in the low THA content hydrogels compared to the high THA content hydrogels. No clear difference was observed related to the Col content. The low THA content hydrogels shrank below the size of the initial diameter (6 mm) on day 7 with a diameter of 3.75 ± 0.46 mm and 3.77 ± 0.24 mm (for 2.5 and 1.7 mg/ml Col respectively) on day 21 (Fig. 2E). On day 7, a larger diameter was measured for high THA content hydrogels than on day 1. The high THA content samples shrank after swelling to 6.09 ± 0.24 mm and 5.4 ± 1.06 mm for 2.5 and 1.7 mg/ml Col respectively on day 21.

3.2. hMSCs chondrogenesis and matrix deposition in THA-Col biomaterials containing hMSC spheroids

hMSC chondrogenic differentiation was assessed through gene expression analysis by RT-qPCR, biochemical assays for DNA and GAG content as well as histological examination to evaluate the effect of THA-Col hydrogels on the pre-cultured hMSC spheroids. The histological stainings show cartilaginous matrix deposition of the embedded hMSCs spheroids in all four material conditions (Fig. 3 A–C, one representative donor is shown). For low THA content hydrogels, migration of the cells within the scaffolds, cell condensation and positive safranin O staining in the sample was visible (Fig. 3A). The initial point of seeding of the hMSC spheroids was hardly visible after three weeks of culture as the cells migrated throughout the hydrogels. For high THA content hydrogels, the initial point of seeding was still visible on day 21. Safranin O positive staining around the area of initial spheroid seeding, as well as cell condensation, was present, but not homogeneously distributed throughout the sample in the high THA content group. This finding matches the reduced cell migration throughout the high THA content hydrogels, which was observed in the brightfield images (Fig. 2A). Collagen II and aggrecan stainings (Fig. 3B-C) were more homogenous distributed in the low THA content hydrogels, compared to the high THA content hydrogels. No clear difference between low and high Col content group was observed.

An increase in GAGs from day 1 to day 21 of culture resulted in all four material groups (Fig. 3D–F). The total amount of GAGs increased most for T12.5-C2.5, namely from 3.131.56 ± 0.62 to 5.95 ± 0.50 µg/sample ($p < 0.0001$), followed by T12.5-C1.7 (1.47 ± 0.46 to 4.10 ± 0.76 µg/sample, $p < 0.0001$), T16.7-C2.5 (1.27 ± 0.59 to 3.96 ± 1.63 µg/sample, $p < 0.0001$) and T16.7-C1.7 (1.44 ± 0.27 to 4.92 ± 1.20 µg/sample, $p < 0.0001$). The total amount of DNA in the samples stayed constant over three weeks of culture. All four THA-Col composites stimulated GAG deposition marked by and increase in GAG/DNA from day 1 to day 21 of culture with the highest GAG/DNA value measured for T16.7-C2.5 on day 21.

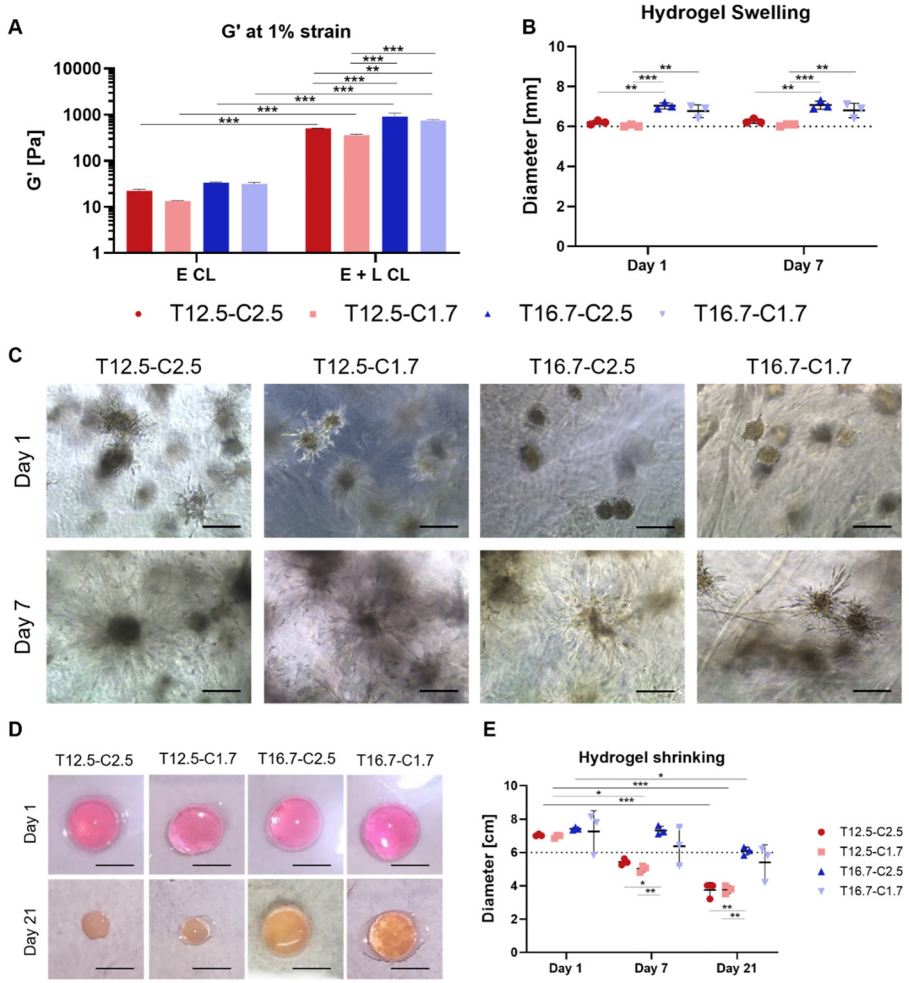

Fig. 2. Material characterization and hMSC migration in 4 different THA-Col formulations (T12.5-C2.5, T12.5-C1.7, T16.7-C2.5, T16.7-C1.7). (A) Storage moduli (G' values) measured at 1% strain of the amplitude sweep of cell-free THA-Col, either enzymatically (E CL) or enzymatically and light (E + L CL) cross-linked. The measurement was performed direct after light cross-linking. N = 3 samples. (B) THA-Col (cell-free) swelling after enzymatic and light cross-linking and subsequent incubation in chondrogenic media (without TGF-β1). Swelling was evaluated by measuring the diameter of the samples (initial diameter: 6 mm). N = 3 samples. (C) Brightfield pictures of hMSC spheroids embedded in THA-Col biomaterials on day 1 and day 7. Scale bar = 100 µm. (D) Macroscopic pictures of THA-Col samples containing hMSC spheroids on day 1 and day 21. Scale bar = 6 mm. (E) Swelling and shrinking of THA-Col samples containing hMSC spheroids during 21 days of culture in chondrogenic media. Swelling and shrinking was evaluated by measuring the diameter of the samples (initial diameter: 6 mm). N = 3 (day 1 and day 21) and N = 2 (day 7) biological replicates, N = 2 technical replicates each, $p < 0.05 = ^{*}$, $p < 0.01 = ^{**}$, $p < 0.001 = ^{***}$.

3.3. Expression of chondrogenic and hypertrophic genes in hMSCs spheroids embedded in THA-Col biomaterials

Gene expression analysis of pre-cultured hMSC spheroids embedded in THA-Col composites showed an upregulation of chondrogenic related markers (Fig. 4A) COL2A1, ACAN and SOX9, indicating chondrogenesis of hMSC spheroids. These genes were upregulated earlier and at higher levels in low THA content hydrogels compared to high THA content hydrogels. In T12.5-C2.5, COL2A1 was up-regulated 2033-fold (p = 0.1086), ACAN 180-fold (p = 0.0746) and SOX9 6-fold (p = 0.0058) after 21 days of culture. The upregulation of the chondrogenic markers in all biomaterial groups on day 21 was comparable to the upregulation of chondrogenic markers in ScMP and SpMP culture (Fig. 6A). Comparing the fibrous and hypertrophic markers (Fig. 4B), the hMSCs embedded in hydrogels expressed COL10A1 to a similarly low level as shown for the hMSCs cultured as SpMP (Fig. 6B). COL1A1 and RUNX2 were slightly down-regulated (0.5 to 0.9-fold), while COL10A1 was slightly upregulated (5 to 15-fold) in all materials on day 21. For low THA content hydrogels, the ratio of COL2A1/COL1A1 (Fig. 4C) increased from day 7 on (T12.5-C2.5: 23-fold,; T12.5-C1.7: 7-fold,; T16.7-C2.5: 0.6-fold,; T16.7-C1.7: 1-fold, all groups p > 0.9999). For high THA content hydrogels the ratios showed an increasing trend only at the later timepoint (T12.5-C2.5: 3375-fold, p = 0.2858; T12.5-C1.7: 1024-fold, p = 0.0043; T16.7-C2.5: 380-fold, p > 0.9999; T16.7-C1.7: 450-fold, p > 0.9999). A similar trend was observed for the COL2A1/COL10A1 (Fig. 4C) ratio, resulting in an increase from day 7 for the low THA content hydrogels (T12.5-C2.5: 10-fold, p > 0.9999; T12.5-C1.7: 4-fold, p > 0.9999; T16.7-C2.5: 0.3-fold, p > 0.9999; T16.7-C1.7: 0.3-fold, p > 0.9999). All hydrogels showed an increase on day 21 (T12.5-C2.5: 163-fold, p = 0.0278; T12.5-C1.7: 109-fold, p = 0.0010; T16.7-C2.5: 39-fold, p = 0.9912; T16.7-C1.7: 17-fold, p > 0.9999). For both ratios, values were higher in low THA compared to high THA hydrogels on day 21.

T12.5-C2.5 showed the most pronounced hMSC chondrogenesis based on the highest level of ECM and GAG deposition, as well as the highest upregulation of chondrogenic markers, followed by T12.5-C1.7. T12.5-C1.7 showed a slightly less pronounced hypertrophic phenotype than T12.5-C2.5, marked by lower expression of hypertrophic markers COL10A1 and RUNX2.

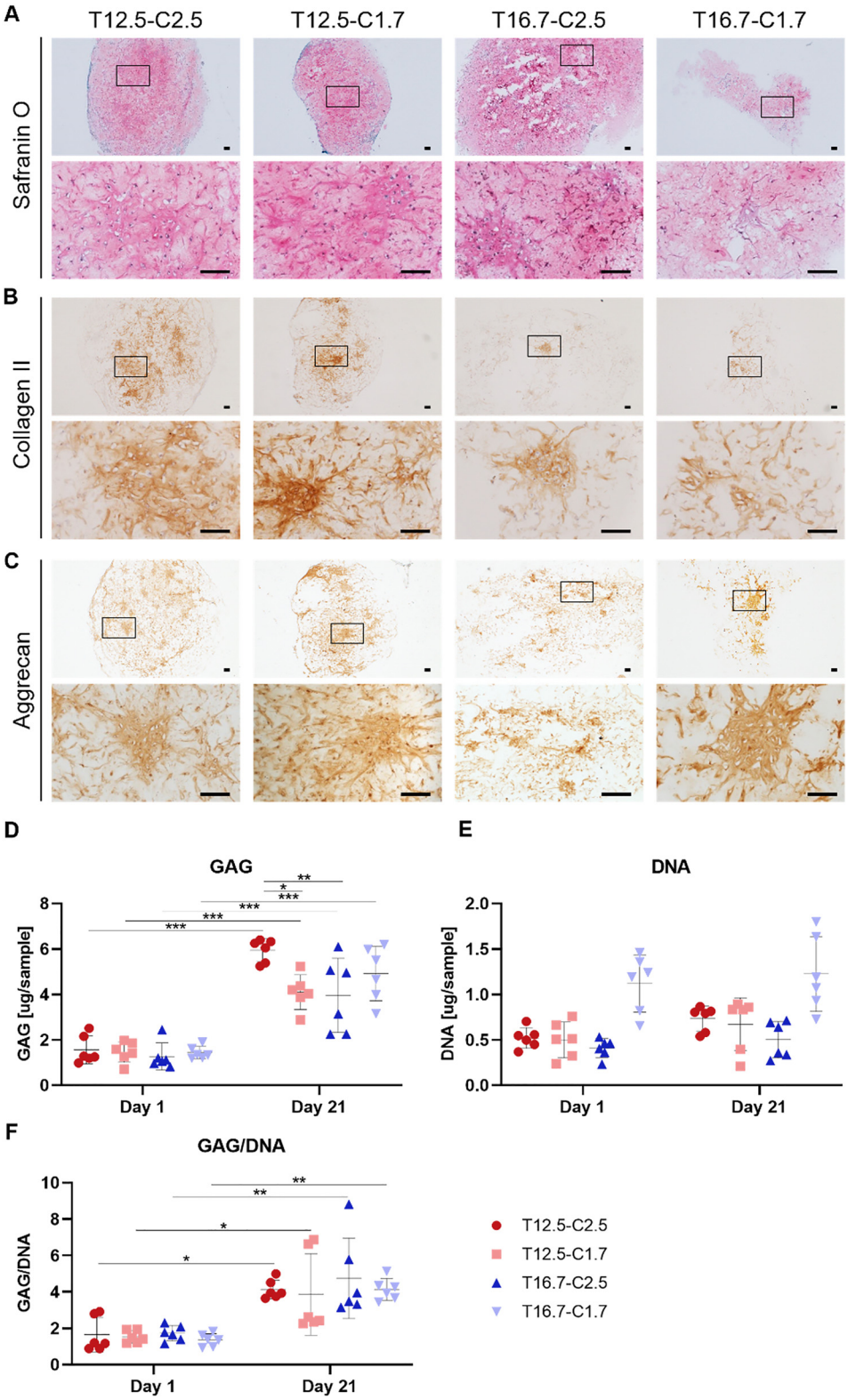

Fig. 3. Chondrogenic differentiation of hMSC spheroids embedded in THA-Col biomaterials at four different polymer concentrations (T12.5-C2.5, T12.5-C1.1, T16.7-C2.5, T16.7-C1.7). (A) Safranin O, (B) collagen II and (C) aggrecan stainings of THA-Col hydrogels containing hMSC spheroids after 21 days of culture. Donor 1 is shown in this figure as representative images for all 3 donors. Scale bar = 100 µm. (D) GAG quantification, (E) DNA quantification and (F) GAG/DNA in THA-Col hydrogels containing hMSC spheroids on day 1 and day 21 of culture. N = 3 biological replicates, N = 2 technical replicates each. $p < 0.05$ = *, $p < 0.01$ = **, $p < 0.001$ = ***.

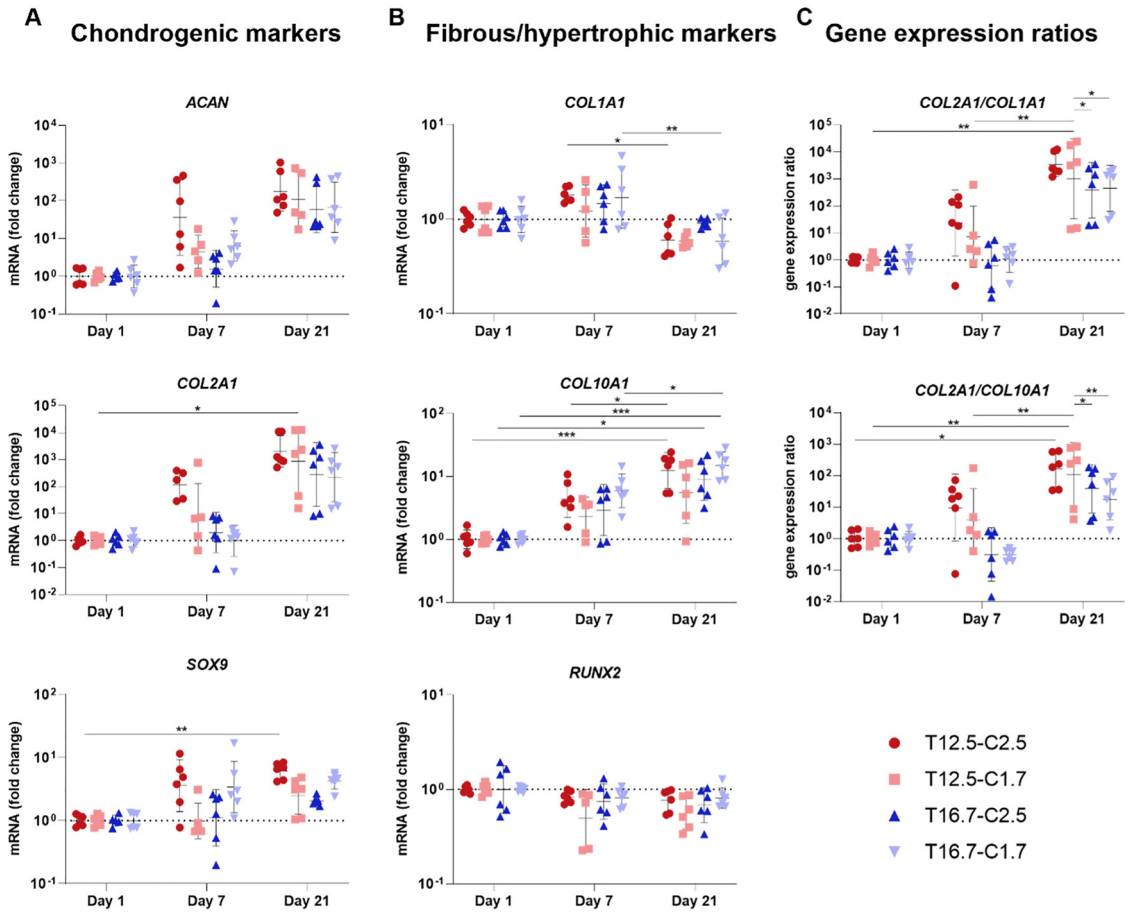

Fig. 4. Gene expression of hMSC spheroids embedded in THA-Col biomaterials at four different THA-Col composites (T12.5-C2.5, T12.5-C1.1, T16.7-C2.5, T16.7-C1.7).(A) Chondrogenic and (B) fibrotic/hypertrophic marker expression in hMSC spheroids embedded in THA-Col biomaterials on day 1, day 7 and day 21. Each point is normalized to the housekeeping gene UBC and to the same condition/donor on day 1. (C) Expression ratios of COL2A1 to COL1A1 and COL2A2 to COL10A1. Geometrical mean and standard deviation are indicated. N = 3 biological replicates, N = 2 technical replicates each. $p < 0.05$ = *, $p < 0.01$ = **, $p < 0.001$ = ***.

3.4. hMSCs chondrogenesis and matrix deposition in SpMP and ScMP pellet cultures

ScMPs (gold standard) and SpMPs were cultured in chondrogenic media containing TGF-β1 to induce chondrogenic differentiation of hMSCs. Cell differentiation was assessed through gene expression analysis by RT-qPCR, biochemical assays for DNA and GAG content as well as (immuno-) histological examination. The histological stainings (Fig. 5A–C) showed cartilaginous matrix deposition in ScMPs and SpMP on day 21, marked by the deposition of GAGs and collagen II. A homogeneous distribution of safranin O positive staining was observed in both culture groups. No clear differences in staining intensity and hMSC morphology were visible comparing the two pellet cultures (Fig. 5A). Immuno-histological stainings showed a homogeneous deposition of matrix rich in collagen II and aggrecan in both pellet cultures (Fig. 5B-C).

At day 21, an increase in GAGs resulted in both SpMP and ScMP groups to a similar extent (SpMP: 1.13 ± 0.33 to 9.46 ± 3.39 µg/pellet, $p < 0.0001$; ScMP: 1.08 ± 0.24 to 9.88 ± 3.88 µg/pellet, $p < 0.0001$). The total amount of DNA in the samples stayed constant over time resulting in an increase in GAG/DNA content on day 21 (SpMP: 1.23 ± 0.45 to 10.03 ± 3.84, $p = 0.0002$; ScMP: 1.25 ± 0.21 to 11.40 ± 3.22, $p < 0.0001$). The ScMPs cultured in chondro-permissive media did not show safranin O positive staining, neither production of retained GAGs in the pellet. However, DNA content in the sample decreased over time, which led to an increase in GAG/DNA from day 1 to day 12 (Fig. 5D–F). Deposition of matrix rich in collagen II or aggrecan was also absent in this control group (Fig. 5A–C).

3.5. Expression of chondrogenic, fibrous and hypertrophic genes in pellet cultures

Gene expression analysis of hMSCs in biomaterials-free SpMP and ScMP culture showed an upregulation of chondrogenic-related markers (Fig. 6A) COL2A1 (SpMP: 1154-fold, $p = 0.1373$; ScMP: 1424-fold, $p = 0.0402$) and ACAN (SpMP: 44-fold, $p = 0.0224$; ScMP: 53-fold, $p = 0.0130$) , confirming chondrogenic differentiation and matrix production to similar extent in both conditions. SOX9 was slightly upregulated on day 7 (SpMP: 3-fold, $p = 0.0856$; ScMP: 5-fold, $p = 0.0006$). The fibrous- and hypertrophic-related markers (Fig. 6B), were less upregulated in the SpMP culture compared to ScMP culture. A slight upregulation of COL1A1 (1-fold vs. 2-fold, $p = 0.0048$) was present on day 7. A similar trend was seen for COL10A1, which was significantly less upregulated in SpMP culture compared to ScMP culture (16-fold vs. 181-fold, $p = 0.0003$) on day 21. The expression of RUNX2 remained unchanged in both conditions. Ratios of COL2A1/COL1A1 and COL2A1/COL10A1 expression were higher in SpMP compared to ScMP culture (COL2A1/COL1A1: 1105-fold vs. 644-fold $p = 0.8640$; COL2A1/COL10A1: 70-fold vs. 8-fold, $p = 0.0259$) (Fig. 6C) on day 21. This indicates a more chondrogenic rather than hypertrophic phenotype in SpMP than ScMP. Gene expression of hMSCs cultured as ScMPs in chondro-permissive media (without TGF-β, Fig. 6A-C)

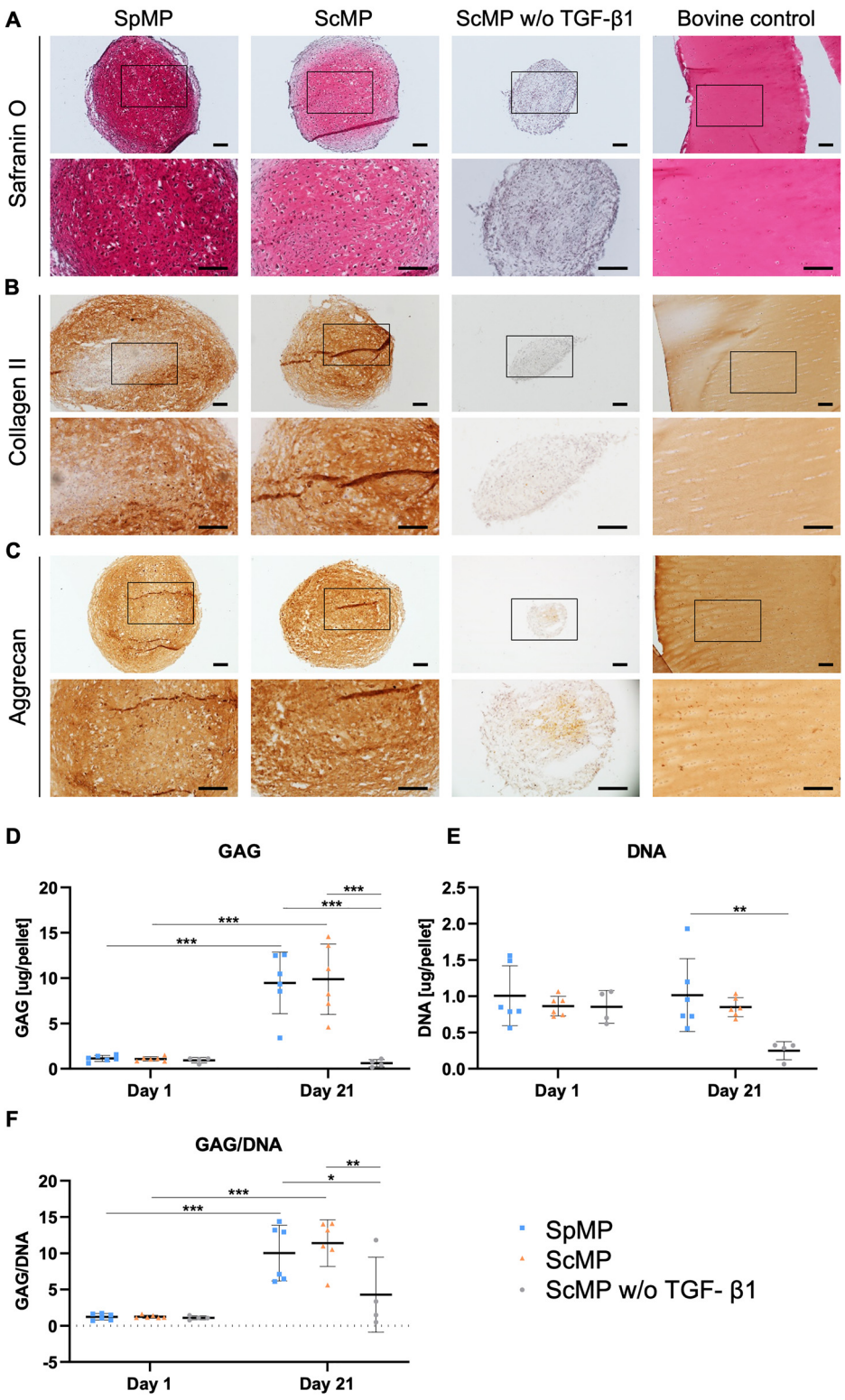

Fig. 5. hMSC chondrogenesis in standard macropellets derived from single cells (ScMP, gold standard) and macropellets derived from hMSC spheroids (SpMP). (A) Safranin O-staining, (B) collagen type II and (C) aggrecan immune-histochemistry of SpMP, ScMP in chondrogenic media. A control of ScMP in chondro-permissive (negative control) media oand bovine articular cartilage control are also shown. Donor 1 is shown as representative result of all 3 donors. Scale bar = 100 µm. (D) GAG quantification, (E) DNA quantification and (F) GAG/DNA in SpMP and ScMP (in chondrogenic and chondro-permissive (negative control) media) on day 1 and day 21 of culture. N = 3 biological replicates, N = 2 technical replicates each. $p < 0.05 = *$, $p < 0.01 = **$, $p < 0.001 = ***$.

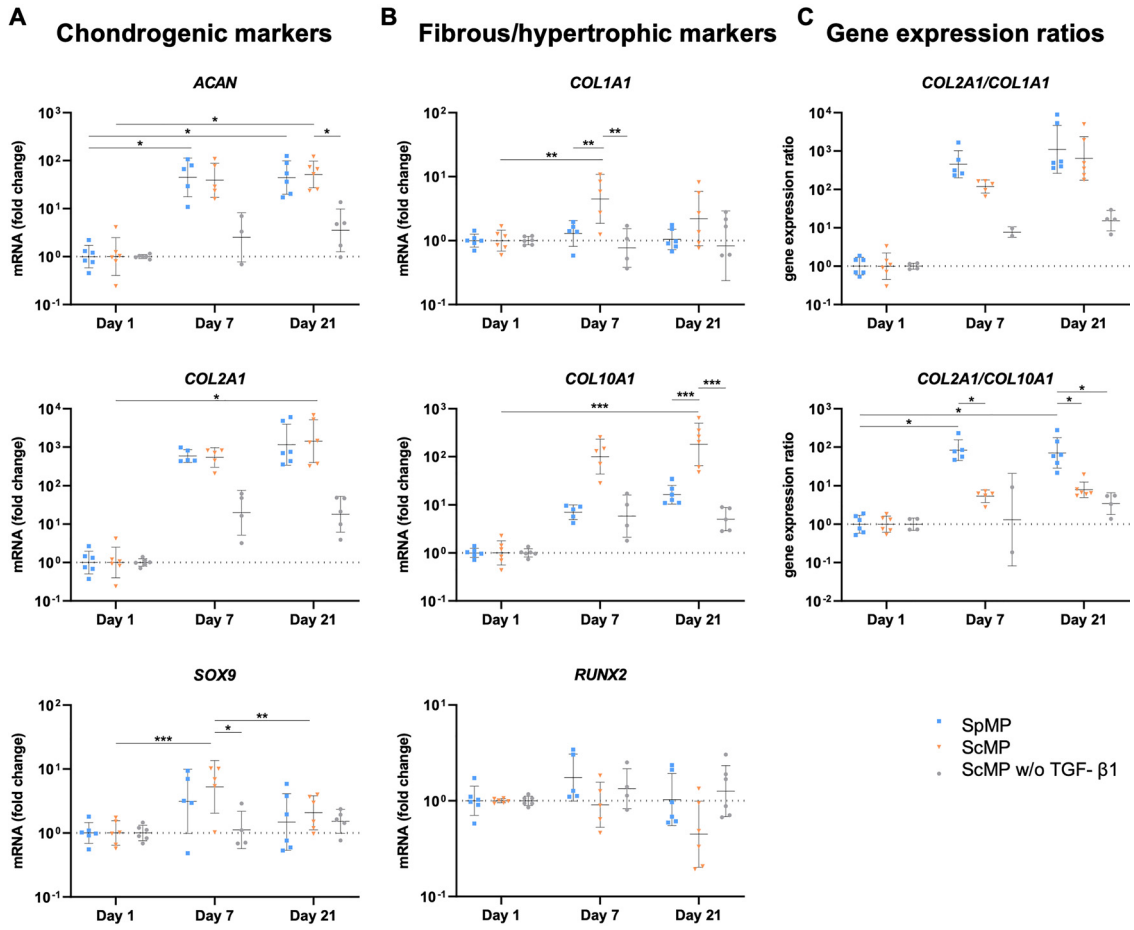

Fig. 6. hMSC chondrogenesis in standard macropellets derived from single cells (ScMP, gold standard) and macropellets derived from hMSC spheroids (SpMP). (A) Chondrogenic and (B) fibrotic/hypertrophic marker expression in SpMP (blue) and ScMP in chondrogenic (orange) and chondro-permissive (negative control; grey) media on day 1, day 7 and day 21. Each point is normalized to the housekeeping gene UBC and to the same condition/donor on day 1. (C) Gene expression ratios of COL2A1 to COL1A1 and COL2A2 to COL10A1. Geometrical mean and geometrical standard deviation are indicated. N = 3 biological replicates, N = 2 technical replicates each. $p < 0.05$ = *, $p < 0.01$ = **, $p < 0.001$ = ***.

showed less upregulation of chondrogenic markers on day 7 and 21 accompanied by slight upregulation of hypertrophic and fibrous markers. This resulted in overall low ratios of fibrous/hypertrophic to chondrogenic markers. The culture of hMSCs in SpMPs induced the same level of hMSC chondrogenesis as culture in ScMPs, while indicating a less upregulation of hypertrophic marker COL10A1.

4. Discussion

hMSC spheroid embedding in 3D biomaterials [33] and the gold standard ScMP culture [12] have shown potential to stimulate cell differentiation and the deposition of cartilaginous ECM after *in vitro* culture. When using biomaterial-based approaches to allow for upscaling and a 3D structure of engineered constructs, the requirement of high cell seeding densities is an obstacle. Despite numerous studies, the driving factors in chondrogenic and hypertrophic differentiation of hMSCs and their modulation through environmental factors like biomaterial composition and cell density are still debated.

In this study, hMSC spheroids were encapsulated in THA-Col biomaterials with the aim to investigate the stimulative effect of the biomaterial composition and polymer content on chondrogenesis and cartilaginous matrix production. hMSC spheroids underwent chondrogenic differentiation after embedding in all four biomaterial formulations. This was indicated by cartilaginous matrix deposition and the expression of chondrogenic genes of spheroids embedded in the biomaterials comparable to those of the SpMP and ScMP culture. hMSCs underwent chondrogenic differentiation despite the relatively low cell density of 5×10^6 cells per ml of hydrogel (4×10^3 spheroids/ml) compared to previous studies which embedded high cell numbers in biomaterials [34]. Chondrogenic differentiation of hMSCs embedded as single cells in hydrogels often require a high cell density in the range of 1-2 $\times$ 10^7 cells/ml [28,35,36] or even up to 10^8 cells/ml [29], depending on the biomaterial used. Our data shows that the embedding of pre-cultured spheroids at 5×10^6 cells/ml was sufficient to induce hMSC chondrogenesis. This was likely due to the initial high cell-cell interaction and cell density within the spheroids. Embedding of hMSCs as spheroids instead of single cells ensures close cell-cell interactions which are required for hMSC condensation, the first step in chondrogenic differentiation [37]. This assumption is supported by clinical data comparing different doses of spheroids for the treatment of cartilage defects (3-7 vs 10-30 vs 40-70 spheroids/cm^2) [7,9]. According to this study, the use of spheroids in cartilage treatment or tissue engineering approaches was less dependent on the overall cell density, but on the cell-cell contacts encountered by the cells.

Despite the intrinsic chondrogenic properties of hyaluronan [38], THA is not supporting hMSC chondrogenesis in absence of Col (see supplementary). This might be related to the lack of integrin-binding sequences, cell migration and thus cell-material interaction in THA compared to THA-Col [39].

Composites with lower THA content of 12.5 mg/ml displayed the highest levels of GAG production, cartilaginous gene expres-

sion, and increased cell migration. This behavior could be putatively attributed to the lower modulus (Fig. 1A). However, given the relatively small difference compared to the formulations with higher THA concentration of 16.7 mg/ml, the difference might also related to other factors such as the different ratios between THA and Col, different stress-relaxation [40] or the increased capability of cells to penetrate constructs with overall lower macromolecular density. In this study, the Col content had only a minor effect on cell response for matching THA concentration. One reason could be that the critical concentration of cell binding motifs was reached at the lower Col concentration tested in this study.

A previous study indicated a different trend with more pronounced chondrogenic differentiation at higher HA and lower gelatin (denatured collagen) content comparing 0/100, 5/95 and 30/70 (%gelatin/%HA) sponges [34]. However, this study was performed with single cells and not with hMSC spheroids, thus the cell-cell interactions and potentially also the interaction of cells with the surrounding material are not comparable [41]. Further, the authors used denatured collagen (gelatin) and no fibrillar collagen. Overall, these findings prove that pre-culture of hMSCs in spheroids are a promising approach to seed cells at an overall low cell densities compared to single cell embedding. This approach also allows to study cell-biomaterial interactions for chondrogenic differentiation. Furthermore, the results of this study showed that hMSC spheroids can be used to assemble microtissues (in our case spheroids) in a biomaterial to create large tissues for cartilage repair, as shown by other groups using similar approaches [42–44]. Currently, chondrocyte pellets without a biomaterial carrier (chondrosphere/Spherox, CO.DON AG) are clinically available to treat large cartilage defects [45]. Compared to this approach, the addition of a biomaterial filler like the THA-Col as we used in our approach could improve the filling of even larger defect volumes and support load transmission. Whether the approach of seeding pre-cultured spheroids into biomaterials is sufficient to fill the void in a large cartilage defect needs to be further investigated *in vivo*.

In parallel to the investigation of the use of spheroids for biomaterial-based cartilage tissue engineering, we studied the effect of hMSC pre-culture in spheroids (250 cells) before aggregation into macropellets (SpMP: 2.5×10^5 cells/SpMP, 10^3 spheroids/SpMP) compared to the standard ScMP culture (2.5×10^5 cells per ScMP). The pre-culture of cells in spheroids before aggregation into SpMP led to a lower upregulation of hypertrophic and fibrotic genes (COL1A1, COL10A1). This was accompanied by higher gene expression ratios for COL2A1/COL10A1 and COL2A1/COL1A1 compared to ScMP culture, indicating a more chondrogenic differentiation of the cells in SpMP than ScMP. The level of chondrogenic marker expression (ACAN, COL2A1, SOX9) and cartilaginous matrix deposition was similar between SpMP and ScMP, indicating that the pre-culture in spheroids did not negatively affect chondrogenic differentiation potential and chondrogenic matrix production. However, it is not fully understood yet to which extent the culture environment may impact the hypertrophic and chondrogenic differentiation *in vitro* [46]. There is evidence that the small size of the hMSC spheroids during the 3 days of pre-culture (250 cells/spheroid) might have a positive effect on the diffusion of TGF-β1 and nutrients, as compared to the ScMP which contains 2.5×10^5 cells from day one of culture. Faster availability of TGF-β1 and nutrients due to smaller size of the construct has been shown to have a positive effect on the cartilaginous matrix deposition and chondrogenic gene expression of hMSC cultures [47]. It has been shown that one day of TGF-β1 exposure is sufficient to direct hMSCs towards chondrogenesis [14], indicating that a fast avilability of TGF-β1 to the cells in the spheroids during pre-culture could play an important role in chondrogenesis at a later stage of culture. Further, our study suggests that the 3 days of pre-culture of hMSCs in small spheroids in media containing TGF-β1 before assembling into a macropellet affects and possibly reduces the expression of hypertrophic genes but does not prevent collagen X expression. However, the role of TGF-β in inhibiting and promoting terminal differentiation of hMSCs has not been fully understood. Some studies show that TGF-β was insufficient to completely prevent hypertrophy in the standard ScMP culture [48,49]. Other studies reported an induction of hypertrophy upon medium supplementation with TGF-β1 [14,50]. Hellingman et al. showed that Smad signalling is likely to control hypertrophic differentiation after 14 days of chondrogenic differentiation in hMSCs. Blocking Smad 1/5/8 or Smad 2/3 phosphorylation prevents hypertrophic gene expression and mineralization in prolonged culture. However, cartilage matrix production was not present when Smad 2/3 phosphorylation was blocked [51].

The reduced Col10A1 expression in our experiments could further be related to the fact that hMSCs in spheroids and thus in SpMPs are less densely packed than in the standard ScMPs and therefore diffusion of TGF-b1 to the cells in the center is faster. This assumption is based on the use of a lower G value when centrifuging the spheroids (100 G) compared to ScMP aggregation (400 G). Further, when SpMPs were centrifuged (400 G), the spheroids already deposited matrix, probably leading to an overall lower cell density after the SpMP generation. This positive effect of lower cell and packing densities was previously investigated by Zhang et al., comparing the chondrogenic and hypertrophic potential of pellet cultures and micromass cultures (self-aggregation of cells in droplets) with the result that micromas cultures led to overall higher chondrogenic differentiation accompanied by lower hypertrophic differentiation [52]. These findings are in line with our data indicating that cell packing density might have an influence on cell differentiation, with the overall trend that a lower density reduces the expression of hypertrophic markers. To understand our findings of reduced hypertrophy in SpMP compared to ScMP culture in more detail, additional experiments analyzing the effect of pellet size, density and TGF-β1 exposure over the course of *in vitro* culture on hypertrophic differentiation are needed. Without further studies, we cannot identify if hypertrophic differentiation was reduced or if gene expression was merely dampened at the evaluated timepoint.

One limitation of this study is the missing comparison of different spheroid sizes or spheroid numbers per construct. Whether the number of spheroids has an impact on matrix production, as it is known for single cells embedded in biomaterials, needs to be addressed in future studies. It would be also of interest to investigate the optimal timing of TGF-β1 exposure, with the overall wish to remove the growth factor stimuli after pre-culture of the spheroids allowing to study biomaterial derived stimuli on chondrogenic matrix deposition. A further limitation is presented by the fact that after 21 days of culture, not the complete hydrogel volume is filled by cells. Therefore, it is not proven yet that seeding microtissues in the form of spheroids can generate a durable tissue.

5. Conclusion

In this work we have shown that pre-culturing hMSC in small spheroids is a promising approach for studying chondrogenic differentiation encapsulated in biomaterials at a relatively low cell count (5×10^6/ml). Comparing different polymer concentrations, we observed increased cell migration, more homogeneous matrix distribution and a more chondrogenic gene expression profile for compositions with lower THA concentration. Pre-culture of spheroids also reduced Col10A1 expression in pellet culture (SpMP) without compromising chondrogenic differentiation and cartilaginous matrix deposition. From a biomaterial point of view, the use of hMSC spheroids overcomes the limitation of limited cell-cell contact of single cells embedded in biomaterials and the optimiza-

tion of cell number for every single biomaterial, thus allowing for screening different biomaterials in the same experiment. The here introduced approach of using hMSC spheroids can be translated to chondrocytes and MSC-chondrocyte co-cultures to study biomaterials free and biomaterials based *in vitro* chondrogenesis, but also cell migration and cell orientation.

Funding

This work is part of the osteochondral defect collaborative research program supported by the AO Foundation. F.S. received the AO Foundation Fellowship in Health Sciences and Technology from ETH Zürich Foundation.

Author contributions

Conceptualization and design: A.S. and F.S., acquisition and analysis: F.S., interpretation of data: F.S., A.S., M.D. and M.S., original draft preparation: F.S. and A.S. revising and editing original draft: A.S., M.D. and M.S., supervision, A.S., M.D., funding acquisition: M.S. and M.D. All authors have read and agreed to the published version of the manuscript.

Declaration of Competing Interest

The authors declare that they have no known competing financial interests or personal relationships that could have appeared to influence the work reported in this paper.

Acknowledgements

This work is part of the osteochondral defect collaborative research program supported by the AO Foundation. The authors acknowledge Dr. med. Sonja Häckl from the Inselspital Basel and PD. Dr. med. David Kubosch from the University Hospital Freiburg for providing human bone marrow samples. Thanks also to Nora Goudsouzian and Mauro Bluvol for their support with histological stainings. The hybridoma and monoclonal antibodies used in the present study was obtained from the Development Hybridoma Bank developed under the auspices of the NICHD and maintained by the University of Iowa, Department of Biological Sciences, Iowa City, IA 52242.

Supplementary materials

Supplementary material associated with this article can be found, in the online version, at doi:10.1016/j.actbio.2022.02.038.

References

[1] E.V. Medvedeva, E.A. Grebenik, S.N. Gornostaeva, V.I. Telpuhov, A.V. Lychagin, P.S. Timashev, A.S. Chagin, Repair of damaged articular cartilage: current approaches and future directions, Int. J. Mol. Sci. 19 (8) (2018).
[2] T.M. Quinn, H.J. Häuselmann, N. Shintani, E.B. Hunziker, Cell and matrix morphology in articular cartilage from adult human knee and ankle joints suggests depth-associated adaptations to biomechanical and anatomical roles, Osteoarthr. Cartil. 21 (12) (2013) 1904–1912.
[3] M.W. Kessler, D.A. Grande, Tissue engineering and cartilage, Organogenesis 4 (1) (2008) 28–32.
[4] Y. Liu, G. Zhou, Y. Cao, Recent progress in cartilage tissue engineering-our experience and future directions, Engineering 3 (2017) 28–35.
[5] A.R. Armiento, M.J. Stoddart, M. Alini, D. Eglin, Biomaterials for articular cartilage tissue engineering: learning from biology, Acta Biomater. 65 (2018) 1–20.
[6] A. Mobasheri, G. Kalamegam, G. Musumeci, M.E. Batt, Chondrocyte and mesenchymal stem cell-based therapies for cartilage repair in osteoarthritis and related orthopaedic conditions, Maturitas 78 (3) (2014) 188–198.
[7] P. Niemeyer, V. Laute, W. Zinser, T. John, C. Becher, P. Diehl, T. Kolombe, J. Fay, R. Siebold, S. Fickert, Safety and efficacy of matrix-associated autologous chondrocyte implantation with spheroid technology is independent of spheroid dose after 4 years, Knee Surg. Sports Traumatol. Arthrosc. 28 (4) (2020) 1130–1143.
[8] C. Eschen, C. Kaps, W. Widuchowski, S. Fickert, W. Zinser, P. Niemeyer, G. Roël, Clinical outcome is significantly better with spheroid-based autologous chondrocyte implantation manufactured with more stringent cell culture criteria, Osteoarthr. Cartil. Open 2 (1) (2020) 100033.
[9] P. Niemeyer, V. Laute, T. John, C. Becher, P. Diehl, T. Kolombe, J. Fay, R. Siebold, M. Niks, S. Fickert, W. Zinser, The effect of cell dose on the early magnetic resonance morphological outcomes of autologous cell implantation for articular cartilage defects in the knee: a randomized clinical trial, Am. J. Sports Med. 44 (8) (2016) 2005–2014.
[10] M.M.J. Caron, P.J. Emans, M.M.E. Coolsen, L. Voss, D.A.M. Surtel, A. Cremers, L.W. van Rhijn, T.J.M. Welting, Redifferentiation of dedifferentiated human articular chondrocytes: comparison of 2D and 3D cultures, Osteoarthr. Cartil. 20 (10) (2012) 1170–1178.
[11] N.P. Grigull, J.I. Redeker, B. Schmitt, M.M. Saller, V. Schönitzer, S. Mayer-Wagner, Chondrogenic potential of pellet culture compared to high-density culture on a bacterial cellulose hydrogel, Int. J. Mol. Sci. 21 (8) (2020).
[12] B. Johnstone, T.M. Hering, A.I. Caplan, V.M. Goldberg, J.U. Yoo, *In vitro* chondrogenesis of bone marrow-derived mesenchymal progenitor cells, Exp.Cell Res. 238 (1) (1998) 265–272.
[13] M. Mueller, R. Tuan, Functional Characterization of Hypertrophy in Chondrogenesis of Human Mesenchymal Stem Cells, Arthr. Rheum. 58 (2008) 1377–1388.
[14] K. Futrega, P. Robey, T. Klein, R. Crawford, M. Doran, A single day of TGF-β1 exposure activates chondrogenic and hypertrophic differentiation pathways in bone marrow-derived stromal cells, Commun. Biol. 4 (2021).
[15] B.D. Markway, G.K. Tan, G. Brooke, J.E. Hudson, J.J. Cooper-White, M.R. Doran, Enhanced Chondrogenic Differentiation of Human Bone Marrow-Derived Mesenchymal Stem Cells in Low Oxygen Environment Micropellet Cultures, Cell Transpl. 19 (1) (2010) 29–42.
[16] S. Chen, P. Fu, R. Cong, H. Wu, P. Md, Strategies to minimize hypertrophy in cartilage engineering and regeneration, Genes Dis. 2 (2015).
[17] J.H. Lee, H.W. Kim, Emerging properties of hydrogels in tissue engineering, J. Tissue Eng. 9 (2018) 204173141876828.
[18] D. Stanco, P. Urbán, S. Tirendi, G. Ciardelli, J. Barrero-Moreno, 3D bioprinting for orthopaedic applications: current advances, challenges and regulatory considerations, Bioprinting 20 (2020).
[19] C. Dong, Y. Lv, Application of collagen scaffold in tissue engineering: recent advances and new perspectives, Polymers 8 (2) (2016).
[20] A. Frayssinet, D. Petta, C. Illoul, B. Haye, A. Markitantova, D. Eglin, G. Mosser, M. D'Este, C. Hélary, Extracellular matrix-mimetic composite hydrogels of cross-linked hyaluronan and fibrillar collagen with tunable properties and ultrastructure, Carbohydr. Polym. 236 (2020) 116042.
[21] V. Irawan, T.C. Sung, A. Higuchi, T. Ikoma, Collagen scaffolds in cartilage tissue engineering and relevant approaches for future development, Tissue Eng. Regen. Med. 15 (2018).
[22] C. Dong, Y. Lv, Application of collagen scaffold in tissue engineering: recent advances and new perspectives, Polymers 8 (2016) 42.
[23] A. Schwab, C. Helary, R.G. Richards, M. Alini, D. Eglin, M. D'Este, Tissue mimetic hyaluronan bioink containing collagen fibers with controlled orientation modulating cell migration and alignment, Mater. Today Bio 7 (2020) 100058.
[24] A. Frayssinet, D. Petta, C. Illoul, B. Haye, A. Markitantova, D. Eglin, G. Mosser, M. D'Este, C. Helary, Extracellular matrix-mimetic composite hydrogels of cross-linked hyaluronan and fibrillar collagen with tunable properties and ultrastructure, Carbohydr. Polym. 236 (2020) 116042.
[25] K.S. Lim, F. Abinzano, P.N. Bernal, A. Albillos Sanchez, P. Atienza-Roca, I.A. Otto, Q.C. Peiffer, M. Matsusaki, T.B.F. Woodfield, J. Malda, R. Levato, One-step photoactivation of a dual-functionalized bioink as cell carrier and cartilage-binding glue for chondral regeneration, Adv. Healthc. Mater. 9 (15) (2020) e1901792.
[26] B.D. Smith, D.A. Grande, The current state of scaffolds for musculoskeletal regenerative applications, Nat. Rev. Rheumatol. 11 (4) (2015) 213–222.
[27] C. Vinatier, J. Guicheux, Cartilage tissue engineering: From biomaterials and stem cells to osteoarthritis treatments, Ann. Phys. Rehabil. Med. 59 (3) (2016) 139–144.
[28] M. Mumme, A. Barbero, S. Miot, A. Wixmerten, S. Feliciano, F. Wolf, A.M. Asnaghi, D. Baumhoer, O. Bieri, M. Kretzschmar, G. Pagenstert, M. Haug, D.J. Schaefer, I. Martin, M. Jakob, Nasal chondrocyte-based engineered autologous cartilage tissue for repair of articular cartilage defects: an observational first-in-human trial, Lancet 388 (10055) (2016) 1985–1994.
[29] S. Talukdar, Q.T. Nguyen, A.C. Chen, R.L. Sah, S.C. Kundu, Effect of initial cell seeding density on 3D-engineered silk fibroin scaffolds for articular cartilage tissue engineering, Biomaterials 32 (34) (2011) 8927–8937.
[30] M. Goldring, K. Tsuchimochi, K. Ijiri, The control of chondrogenesis, J. Cell. Biochem. 97 (2006) 33–44.
[31] C. Loebel, M. D'Este, M. Alini, M. Zenobi-Wong, D. Eglin, Precise tailoring of tyramine-based hyaluronan hydrogel properties using DMTMM conjugation, Carbohydr. Polym. 115 (2015) 325–333.
[32] O. Gardner, M. Alini, M. Stoddart, Mesenchymal stem cells derived from human bone marrow, 2015, pp. 41-52.
[33] V. Rai, M. Dilisio, N. Dietz, D. Agrawal, Recent strategies in cartilage repair: a systemic review of the scaffold development and tissue engineering, J. Biomed. Mater. Res. Part A (2017) 105.
[34] C.G. Pfeifer, A. Berner, M. Koch, W. Krutsch, R. Kujat, P. Angele, M. Nerlich, J. Zellner, Higher ratios of hyaluronic acid enhance chondrogenic differentiation of human MSCs in a hyaluronic acid–gelatin composite scaffold, Materials 9 (5) (2016).
[35] J. Hauptstein, T. Böck, M. Bartolf-Kopp, L. Forster, P. Stahlhut, A. Nadernezhad, G. Blahetek, A. Zernecke-Madsen, R. Detsch, T. Jüngst, J. Groll, J. Teßmar,

T. Blunk, Hyaluronic acid-based bioink composition enabling 3D bioprinting and improving quality of deposited cartilaginous extracellular matrix, Adv. Healthc. Mater. 9 (15) (2020) 2000737.
[36] Z. Li, L. Kupcsik, S.J. Yao, M. Alini, M.J. Stoddart, Chondrogenesis of human bone marrow mesenchymal stem cells in fibrin-polyurethane composites, Tissue Eng. Part A 15 (7) (2009) 1729–1737.
[37] S. Boeuf, W. Richter, Chondrogenesis of mesenchymal stem cells: role of tissue source and inducing factors, Stem Cell Res. Ther. 1 (4) (2010) 31.
[38] E. Amann, P. Wolff, E. Breel, M. van Griensven, E.R. Balmayor, Hyaluronic acid facilitates chondrogenesis and matrix deposition of human adipose derived mesenchymal stem cells and human chondrocytes co-cultures, Acta Biomater. 52 (2017) 130–144.
[39] A. Schwab, C. Helary, R. Richards, M. Alini, D. Eglin, M. D'Este, Tissue mimetic hyaluronan bioink containing collagen fibers with controlled orientation modulating cell migration and alignment, Mater. Today Bio 7 (2020) 100058.
[40] O. Chaudhuri, L. Gu, D. Klumpers, M. Darnell, S.A. Bencherif, J.C. Weaver, N. Huebsch, H.P. Lee, E. Lippens, G.N. Duda, D.J. Mooney, Hydrogels with tunable stress relaxation regulate stem cell fate and activity, Nat. Mater. 15 (3) (2016) 326–334.
[41] S.J. Kim, E.M. Kim, M. Yamamoto, H. Park, H. Shin, Engineering multi-cellular spheroids for tissue engineering and regenerative medicine, Adv. Healthc. Mater. (2020) e2000608.
[42] B.S. Schon, G.J. Hooper, T.B.F. Woodfield, Modular tissue assembly strategies for biofabrication of engineered cartilage, Ann. Biomed. Eng. 45 (1) (2017) 100–114.
[43] B.K. Babur, K. Futrega, W.B. Lott, T.J. Klein, J. Cooper-White, M.R. Doran, High-throughput bone and cartilage micropellet manufacture, followed by assembly of micropellets into biphasic osteochondral tissue, Cell Tissue Res 361 (3) (2015) 755–768.
[44] J. Wei, P. Ran, Q. Li, J. Lu, L. Zhao, Y. Liu, X. Li, Hierarchically structured injectable hydrogels with loaded cell spheroids for cartilage repairing and osteoarthritis treatment, Chem. Eng. J. 430 (2022) 132211.
[45] P. Niemeyer, V. Laute, W. Zinser, T. John, C. Becher, P. Diehl, T. Kolombe, J. Fay, R. Siebold, S. Fickert, Safety and efficacy of matrix-associated autologous chondrocyte implantation with spheroid technology is independent of spheroid dose after 4 years, Knee Surg. Sports Traumatol. Arthrosc. 28 (4) (2020) 1130–1143.
[46] D. Studer, C. Millan, E. Öztürk, K. Maniura, M. Zenobi, Molecular and biophysical mechanisms regulating hypertrophic differentiation in chondrocytes and mesenchymal stem cells, Eur. Mater. 24 (2012) 118–135 discussion 135.
[47] A.D. Murdoch, L.M. Grady, M.P. Ablett, T. Katopodi, R.S. Meadows, T.E. Hardingham, Chondrogenic differentiation of human bone marrow stem cells in transwell cultures: generation of scaffold-free cartilage, Stem Cells 25 (11) (2007) 2786–2796.
[48] M.B. Mueller, M. Fischer, J. Zellner, A. Berner, T. Dienstknecht, L. Prantl, R. Kujat, M. Nerlich, R.S. Tuan, P. Angele, Hypertrophy in mesenchymal stem cell chondrogenesis: effect of TGF-beta isoforms and chondrogenic conditioning, Cells Tissues Organs 192 (3) (2010) 158–166.
[49] I. Sekiya, J.T. Vuoristo, B.L. Larson, D.J. Prockop, *In vitro* cartilage formation by human adult stem cells from bone marrow stroma defines the sequence of cellular and molecular events during chondrogenesis, Proc. Natl. Acad. Sci. U. S. A. 99 (7) (2002) 4397–4402.
[50] R. Narcisi, R. Quarto, V. Ulivi, A. Muraglia, L. Molfetta, P. Giannoni, TGF β-1 administration during *Ex vivo* expansion of human articular chondrocytes in a serum-free medium redirects the cell phenotype toward hypertrophy, J. Cell. Physiol. 227 (2012) 3282–3290.
[51] C.A. Hellingman, W. Koevoet, G.J. van Osch, Can one generate stable hyaline cartilage from adult mesenchymal stem cells? A developmental approach, J. Tissue Eng. Regen. Med. 6 (10) (2012) e1–e11.
[52] L. Zhang, P. Su, C. Xu, J. Yang, W. Yu, D. Huang, Chondrogenic differentiation of human mesenchymal stem cells: a comparison between micromass and pellet culture systems, Biotechnol. Lett. 32 (9) (2010) 1339–1346.